JOURNAL OF
biomaterials applications

Journal of Biomaterials Applications
2015, Vol. 29(6) 837–853

DOI: 10.1177/0885328214546647
jba.sagepub.com
SAGE

Effects of fiber density and plasma modification of nanofibrous membranes on the adhesion and growth of HaCaT keratinocytes

Marketa Bacakova[1], Frantisek Lopot[2], Daniel Hadraba[1,2], Marian Varga[3], Margit Zaloudkova[4], Denisa Stranska[5], Tomas Suchy[4] and Lucie Bacakova[1]

Abstract

It may be possible to regulate the cell colonization of biodegradable polymer nanofibrous membranes by plasma treatment and by the density of the fibers. To test this hypothesis, nanofibrous membranes of different fiber densities were treated by oxygen plasma with a range of plasma power and exposure times. Scanning electron microscopy and mechanical tests showed significant modification of nanofibers after plasma treatment. The intensity of the fiber modification increased with plasma power and exposure time. The exposure time seemed to have a stronger effect on modifying the fiber. The mechanical behavior of the membranes was influenced by the plasma treatment, the fiber density, and their dry or wet state. Plasma treatment increased the membrane stiffness; however, the membranes became more brittle. Wet membranes displayed significantly lower stiffness than dry membranes. X-ray photoelectron spectroscopy (XPS) analysis showed a slight increase in oxygen-containing groups on the membrane surface after plasma treatment. Plasma treatment enhanced the adhesion and growth of HaCaT keratinocytes on nanofibrous membranes. The cells adhered and grew preferentially on membranes of lower fiber densities, probably due to the larger area of void spaces between the fibers.

Keywords

Tissue engineering, nanofibers, needle-less electrospinning, fiber density, plasma-treatment, skin, fibroblasts, keratinocytes

Introduction

Nanofibrous materials are being applied increasingly in tissue engineering, because they can better mimic the structure and the mechanical properties of the fibrous components of natural extracellular matrix (ECM). For this reason, they are considered to be attractive for adhesion and growth of cells. In comparison with conventionally used flat or microstructured surfaces, nanostructured materials enhance the cell–material interaction. This enhancement is due to the adsorption of cell adhesion-mediating ECM molecules from biological fluids in an appropriate spatial conformation. This enables good accessibility of specific sites on these molecules for cell adhesion receptors.[1,2] In addition, nanofibrous membranes are advantageous for constructing the bilayer of skin cells – fibroblasts and keratinocytes – in skin tissue engineering. These membranes will separate the two cell types, but due to the porous structure of the material, they will ensure their physical and humoral communication. The layer of fibroblasts can therefore serve as a nutrient feeder for keratinocytes, similarly as in the native skin.[3]

[1]Institute of Physiology, Academy of Sciences of the Czech Republic, Czech Republic
[2]Dept. of Anatomy and Biomechanics, Faculty of Physical Education and Sport, Charles University, Czech Republic
[3]Institute of Physics, Academy of Sciences of the Czech Republic, Czech Republic
[4]Institute of Rock Structure and Mechanics, Academy of Sciences of the Czech Republic, Czech Republic
[5]Elmarco Ltd., Czech Republic

Corresponding author:
Marketa Bacakova, MSc., Institute of Physiology, Academy of Sciences of the Czech Republic, Videnska 1083, Prague 4 14220, Czech Republic.
Email: marketa.bacakova@biomed.cas.cz

Various artificial and natural materials have been adopted for constructing a scaffold that is suitable for treating skin injuries. Artificial skin substitutes can be made from poly(HEMA),[4,5] polybuthylene terephthalate,[6] nylon,[7,8] hydroxybuthyrate,[9] polycaprolactone,[10] polylactic acid,[11] and polyglycolic acid, or their copolymers.[11,12] The most widely tested and applied natural biomaterials are chitosan,[13,14] collagen,[15] hyaluronic acid,[16,17] and chondroitin sulfate.[18] For our study, we used biodegradable nanofibrous membranes made from polylactic acid (polylactide, PLA). The main advantage of biodegradable materials is their slow resorption in the organism, associated with a decrease in molecular weight. In the case of PLA, this decrease in molecular weight is due to the transformation of polylactide to lactide by hydrolysis of aliphatic ester linkages in PLA molecules.[19] The lactic acid is further metabolized and removed from the body as carbon monoxide and water. Due to their ability to be resorbed, biodegradable materials are finally replaced by regenerated tissue.

Generally, materials used in tissue engineering have to be biocompatible. They cannot be cytotoxic, mutagenic or immunogenic, and their physical and chemical properties should correspond to the properties of the replaced tissue. In advanced tissue engineering, biomaterials used for bioartificial tissue substitutes should be bioactive. They should act as analogs of the natural ECM, i.e. they should promote and control the adhesion, proliferation, differentiation, and maturation of cells, and thus the regeneration of damaged tissue. The bioactivity of materials depends strongly on the physical and chemical properties of the material surface, such as its wettability, electrical charge and conductivity, mechanical properties, surface roughness, and topography. For this reason, some materials do not have optimal physical and chemical properties for fully replacing damaged tissue, and need further modification. These further modifications should enhance cell–material interaction and the formation of new tissue (for a review, see Bacakova et al.[1] and Bacakova and Svorcik[20]).

The physical and chemical properties of the polymer surface can be altered by several physical techniques, particularly by irradiation with an ion beam,[21,22] ultraviolet light,[23] or exposure to plasma discharge.[24–26] The common feature of these techniques is the induction of polymer chain degradation, the creation of free radicals and double bonds, and crosslinking of the polymer chains. These radicals react with oxygen in the ambient atmosphere, leading to the formation of oxygen-containing chemical groups on the material surface (i.e. carbonyl, carboxyl, hydroxyl, ether, or ester groups). The oxygen groups enhance the polarity and wettability of the material and promote the adsorption of cell adhesion-mediating molecules in an appropriate spatial conformation. This enhancement guarantees that the specific amino acid sequences of these molecules are well accessible for cell adhesion receptors – integrins. In addition, conjugated double bonds between carbon atoms are created during plasma treatment, and this influences the electrical conductivity of the polymer surface. It is known that electrical conductivity of the material surface enhances cell colonization.[1]

In this study, we have evaluated the adhesion and growth of immortal human HaCaT keratinocytes on polylactide nanofibrous membranes modified in oxygen plasma under various process conditions. The aim of this modification was to create a nanofibrous membrane surface that would be attractive for keratinocyte colonization. These plasma-treated membranes could be used as temporary carriers for skin cells during wound healing after skin injury.

Materials and methods

Preparation and modification of nanofibrous membranes

Poly(L-lactide) (PLA, Ingeo™ Biopolymer 4032D) was purchased from NatureWorks, Minnetonka, MN, USA. The molecular parameters of the polymer material, determined by size exclusion chromatography, were $M_w = 124{,}000$ g/mol and $M_n = 48{,}000$ g/mol.[27] A 7 wt.% solution of PLA in a mixture of chloroform, dichloroethane, and ethyl acetate was used for the electrospinning process. First, the polymer was diluted only in chloroform, and the two other solvents were added after the dilution. The polymer solution was made electrically conductive with the use of tetraethylammonium bromide, which was first dissolved in dimethylformamide at a concentration of 3 wt.%, and then 3 g of this solution was added to 100 g of the PLA solution.

Nanofibrous membranes were prepared using the novel Nanospider needleless electrospinning technology (NS Lab 500, Elmarco Ltd., Liberec, Czech Republic). The process conditions were: electrode distance: 180 mm; voltage: 60–10 kV; the spinning electrode rotated at 4 rpm; relative humidity: 25–30%, and room temperature. The membranes were prepared at various fiber densities, i.e. the area weight of the prepared nanofibers was 5, 9, 16, 30 g/m^2.

The membranes were then treated by oxygen plasma discharge using the Phantom LT CCP-RIE System, Trion Technology, in two steps. The first step was performed in etching regime with discharge power from 25 W to 100 W, exposure time from 10 s to 120 s, pressure 150 mTorr, and oxygen flow 20 cm^3/s. The first step was followed by blowing the device (second step)

for 30 s with pressure 150 mTorr and argon flow 20 cm^3/s. The nanofibrous membranes were treated on both sides.

Characterization of the physical and chemical properties of nanofibrous membranes

The morphology of the nanofibrous membranes before and after plasma treatment was evaluated by scanning electron microscopy (SEM) using an SEM field-emission gun operating in secondary electron mode (FE-SEM Tescan MIRA3). The diameter of the fibers and the area of the void spaces among the fibers were measured on the SEM images using Atlas software (Tescan Ltd., Brno, Czech Republic). The diameter of the fibers was expressed in nm, and the area of the void spaces among the fibers was expressed in μm^2.

The mechanical properties of the plasma-treated membranes (plasma power 75 W, exposure time 30 s) and the non-treated nanofibrous membranes of two different fiber densities (5 and 16 g/m^2) were tested in the dry state (at normal air atmosphere and room temperature) and in the wet state, i.e. in phosphate-buffered saline (PBS) at room temperature. The uniaxial tensile test was selected because the SEM images had proven isotropy of the materials. The rectangular strips of constant geometry were fastened into the tensile instrument and were stretched at a constant speed of 6 mm/s. The elongation and force were recorded by sampling frequency 20 Hz and calculated into the stress–strain curve. Finally, the Young's modulus was established for each material and condition. The difference between the groups was statistically evaluated by the two-sample *t*-test.

The chemical composition (concentration of oxygen, carbon, and C–C, C–O, C = O) of the membrane surface before and after plasma treatment was determined by X-ray photoelectron spectroscopy (XPS), using an ADES-400 photoelectron spectrometer (V. G. Scientific, UK). The concentration was determined in at.% with sensitivity 0.1 at.%.

Cell culture on nanofibrous membranes

The nanofibrous membranes were cut into square samples (1 × 1 cm) and were fixed in CellCrown inserts (Scaffdex Ltd., Finland). The samples were sterilized in 70% ethanol for 30 min. After sterilization, the samples were rinsed in distilled water for one week to remove residues of the solvents used during the preparation of the nanofibers. The water was changed every day.

The samples fixed in CellCrown inserts were inserted into polystyrene 24-well cell culture plates (TPP, Switzerland, well diameter 1.5 cm). The samples were seeded with human HaCaT keratinocytes[28] (CLS Cell Lines Service) at a density of 30,000 cells per well (i.e. 15,000 cells/cm^2) into 1.5 ml Dulbecco's modified Eagle's Medium (DMEM; Sigma-Aldrich, USA) with 10% of fetal bovine serum (FBS; Sebak GmbH, Germany) and 40 μg/ml of gentamicin (LEK, Slovenia). The cells were cultivated for 1, 3, and 7 days in a cell incubator at 37°C and in a humidified atmosphere with 5% of CO_2 in the air.

Evaluation of cell growth and mitochondrial activity on nanofibrous membranes

On days 1, 3, and 7 after seeding, the number of initially adhered cells and their subsequent growth on the samples were estimated by the amount of cellular DNA, using the Picogreen dsDNA assay kit (Invitrogen®). The assay is based on measurements of the fluorescence of Picogreen, a nucleic acid stain for quantitating double-stranded DNA in solution. The assay was carried out according to the manufacturer's protocol. Fluorescence was measured with the Synergy HT Multi-Mode Reader (BioTek, USA) in black 96-well cell culture plates (96 F Nunclon delta, Black microwell Si) with excitation wavelength of 480 nm and emission wavelength of 520 nm. The amount of cell DNA on each sample in all time intervals was expressed in ng/cm^2.

Cell mitochondrial activity was measured on days 3 and 7 after seeding by the XTT Cell Proliferation Kit (Roche). The principle of this assay is the cleavage of yellow tetrazolium salt XTT to form a water-soluble orange formazan salt by metabolic cell activity. The formazan dye was then quantified by monitoring the absorbance using a spectrophotometer (ELISA reader). The assay was performed according to the manufacturer's protocol. The absorbance was measured using the VersaMax ELISA Microplate Reader (Molecular Devices Corporation, Sunnyvale, CA, USA) in 96-well cell culture plates (F 96 Maxisorp (NUNC –Imunoplate)) with wavelength 470 nm.

For both analyses (the Picogreen assay and the XTT assay), the samples of nanofibrous membranes were moved into unused fresh 24-well plates to avoid the influence of the cells adhered to the bottom of the wells.

Evaluation of cell adhesion, spreading and morphology on nanofibrous membranes

The spreading and the morphology of the cells on the PLA nanofibers were visualized on days 1, 3, and 7 after seeding by staining the cells with a combination of fluorescent dyes (Hoechst #33342 cell nucleus dye, Texas Red C_2-maleimide cell membrane dye) and with scanning electron microscopy (SEM).

For staining the cells with a combination of fluorescent dyes, the cells were rinsed with PBS, fixed with cold (−20°C) 70% ethanol for 10 min, and then stained for 1 h at room temperature with a combination of fluorescent dyes diluted in PBS: Hoechst #33342 cell nucleus dye (Sigma-Aldrich, 5 μg/ml) and Texas Red C_2-maleimide cell membrane dye (Molecular Probes, Invitrogen, 20 ng/ml). Images documenting the cell morphology were taken using an epifluorescence microscope (Olympus IX 51, Japan, obj. 10×) equipped with a digital camera (DP 70, Japan). The cell cluster spreading area (in μm^2) was measured in the images, which were acquired under a fluorescence microscope using Atlas software (Tescan Ltd., Brno, Czech Republic) on day 3 after seeding.

For SEM, the samples were fixed in 3% glutaraldehyde in PBS, washed with PBS buffer, dehydrated in an ethanol series (25, 50, 75, 90, 96 and 100% v/v), transferred to 100% (v/v) acetone, and dried in a BALZERS CPD 010 critical-point dryer. The samples were then sputter-coated with gold and examined with a Quanta 450 scanning electron microscope (FEI, USA). The high vacuum mode was used, and images were taken on an ETD – Everhart-Thornley detector in secondary electrons mode at high voltage 20 kV, magnification 2000×.

Immunofluorescence staining of molecules participating in cell differentiation, adhesion, and spreading

On day 3 after seeding, the presence of the following markers in HaCaT cells was evaluated:

- keratin 5 and filaggrin as early and middle differentiation markers of keratinocytes
- $ß_1$ integrin, an important molecule for mediating cell–material interaction
- vinculin, an integrin-associated protein present in focal adhesion plaques
- F-actin, an important component of the cell cytoplasmic cytoskeleton associated with focal adhesion plaques.

For immunofluorescence staining of keratin 5, filaggrin, $ß_1$ integrin, and vinculin, the cells were rinsed in PBS and fixed with cold (−20°C) 70% ethanol for 10 min at room temperature. After fixation, the cells were treated with 1% bovine serum albumin in PBS containing 0.05% Triton X-100 (Sigma-Aldrich) for 20 min, and then with 1% Tween (Sigma-Aldrich) in PBS for 20 min at room temperature to block nonspecific binding sites and to permeabilize the cell membrane. The cells were then incubated with the following primary monoclonal antibodies overnight at 4°C: basal cell cytokeratin (RCK 103, mouse, MUbioBV), anti-filaggrin (rabbit, Sigma-Aldrich), anti-$ß_1$ integrin (mouse, Millipore), and anti-vinculin (mouse, Sigma-Aldrich). All antibodies were diluted in PBS to a concentration of 1:200. After rinsing with PBS, the secondary antibody, i.e. goat anti-mouse F(ab′)2 fragments of IgG (H + L) or goat anti-rabbit F(ab′)2 fragments of IgG (H + L), conjugated with Alexa Fluor® 488 (Molecular Probes, Invitrogen), was diluted in PBS to a ratio of 1:400 and applied to the samples for 1 h at room temperature in the dark. The cells were rinsed with PBS and scanned using a Leica TCS SPE DM2500 upright confocal microscope, obj. 63 × / 1.3 NA oil.

F-actin, an important component of the cell cytoplasmic cytoskeleton, was stained with phalloidin conjugated with TRITC (Sigma-Aldrich) diluted in PBS to a final concentration of 5 μg/ml for 1 h at room temperature, after rinsing the cells in PBS and fixation with 70% ethanol (−20°C, 10 min). The actin cytoskeleton was imaged using a Leica TCS SPE DM2500 upright confocal microscope, obj. 63 ×/1.3 NA oil.

Statistics

If not stated otherwise in the text above, the quantitative data are presented as mean ± standard error of mean (S.E.M.) or as mean ± standard deviation (SD) from three independent samples for each experimental group and time interval. Statistical significance was evaluated using the analysis of variance, Student–Newman–Keuls method. Values of $p \leq 0.05$ were considered as significant.

Results

Physical and chemical properties of polylactide nanofibrous membranes

The morphology of nanofibrous membranes of four different fiber densities (5 g/m^2, 9 g/m^2, 16 g/m^2, and 30 g/m^2), and the potential fiber modification and degradation after plasma treatment were investigated by scanning electron microscopy (SEM). The nanofibrous membranes consisted of mostly straight and randomly oriented fibers. The thickest fibers were measured on membranes with density of fibers 30 g/m^2 in the non-treated state and also in the plasma-treated state. The area of the void spaces between fibers decreased with the density of the fibers. After plasma treatment, the fiber diameter did not change, or increased slightly and insignificantly; however, the area of the void spaces between the fibers decreased significantly (Table 1).

The SEM images show significant modification of the nanofibers after plasma treatment. The membranes

Table 1. Morphological parameters of PLA membranes of various fiber densities (5 g/m^2, 9 g/m^2, 16 g/m^2 and 30 g/m^2) before and after plasma treatment.

Treatment	Density of fibers (g/m^2)	5	9	16	30
	Fibers				
Non-treated	Diameter, range (nm)	63 to 927	40 to 763	40 to 799	80 to 1073
	Diameter, mean ± S.E.M (nm)	287.0 ± 13.4	218.6 ± 10.2	271.1 ± 10.9	333.9 ± 10.4
Plasma-treated	Diameter, range (nm)	80 to 1107	63 to 701	63 to 847	80 to 1087
	Diameter, mean ± S.E.M (nm)	287.5 ± 13.2	241.5 ± 9.9	276.3 ± 12.9	339.4 ± 19.4
	Void spaces				
Non-treated	Area, range (μm2)	0.09 to 7.29	0.09 to 5.31	0.08 to 4.52	0.1 to 3.16
	Area, mean ± S.E.M (μm2)	1.64 ± 0.11	1.04 ± 0.08	0.90 ± 0.06	0.76 ± 0.05
Plasma-treated	Area, range (μm2)	0.05 to 4.68	0.1 to 3.37	0.07 to 3.57	0.04 to 2.6
	Area, mean ± S.E.M (μm2)	1.28 ± 0.10*	0.77 ± 0.05*	0.63 ± 0.05*	0.43 ± 0.03*

Note: Mean ± S.E.M. from 127 to 215 measurements (fibers) and 131 to 196 measurements (void spaces). ANOVA, Student–Newman–Keuls method. Statistical significance: *$p \leq 0.05$ in comparison with non-treated samples.

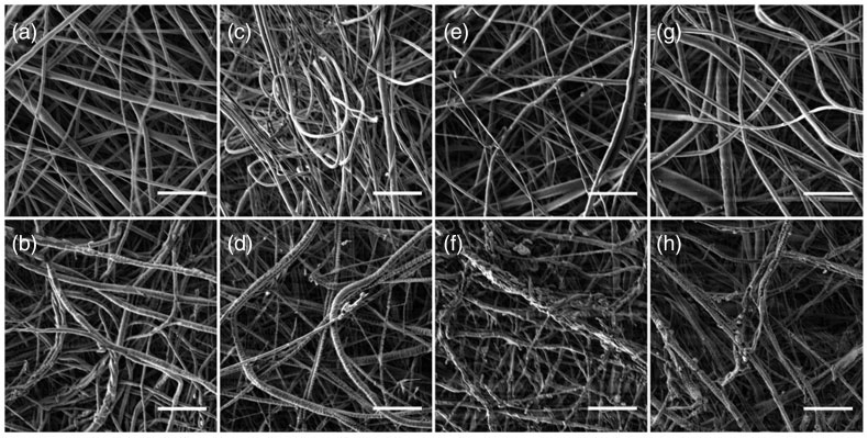

Figure 1. SEM images of PLA membranes of various fiber densities (a, b: 5 g/m^2; c, d: 9 g/m^2; e, f: 16 g/m^2; g, h: 30 g/m^2) before (a, c, e, g) and after the plasma treatment with power 75 W and exposure time 30 s (b, d, f, h). FE-SEM Tescan MIRA3, magnification 10,000×, bar 5 μm.

of higher fiber densities (16 g/m^2 and 30 g/m^2) showed more pronounced modification of the fibers than the membranes of lower fiber densities (5 g/m^2 and 9 g/m^2) after plasma treatment with power 75 W and exposure time 30 s. The fibers in membranes of higher fiber densities seemed to be more degraded than the fibers in membranes of lower fiber densities (Figure 1). We also investigated the influence of various powers and exposure times on the modification of the nanofibers. When low power (25–50 W) and a short exposure time (10–30 s) were used, there was no modification of the fibers (Figure 2). However, if higher power (50–100 W) with a longer exposure time (30–120 s) was applied, modification of the fibers was clearly apparent in the membranes (Figure 3). The SEM data show that the fiber modification increased with power and exposure time. The plasma exposure time seemed to have a more significant effect than the plasma power on fiber modification. For example, nanofibrous membranes treated in plasma with lower power 50 W for a longer exposure time 60 s (Figure 3c) or 120 s (Figure 3d) showed stronger fiber modification and also significant degradation of fibers in a deeper layer of the membrane than membranes treated with higher power 75 W (Figure 3e) or 100 W (Figure 3f) for a shorter exposure time of 30 s (Figure 3(e) and (f)).

We characterized the mechanical properties of the membranes in order to investigate the response of nanofibrous membranes to mechanical stress generated mainly by cell activity (i.e. adhesion, spreading, migration, etc.). The mechanical behavior of the membranes was influenced by fiber density (5 and 16 g/m^2),

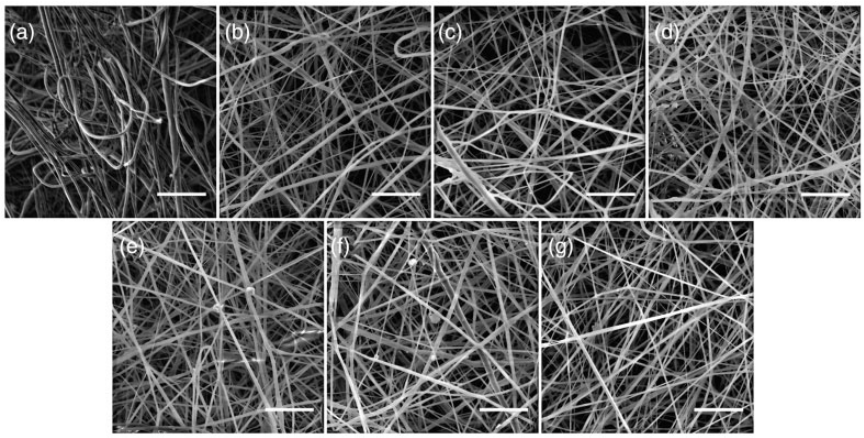

Figure 2. SEM images of PLA membranes of fiber density 9 g/m^2 before (a) and after plasma treatment with various power and exposure times: (b) 25 W 10 s, (c) 25 W 20 s, (d) 25 W 30 s, (e) 50 W 10 s, (f) 50 W 20 s, (g) 50 W 30 s. FE-SEM Tescan MIRA3, magnification 10,000×, bar 5 μm.

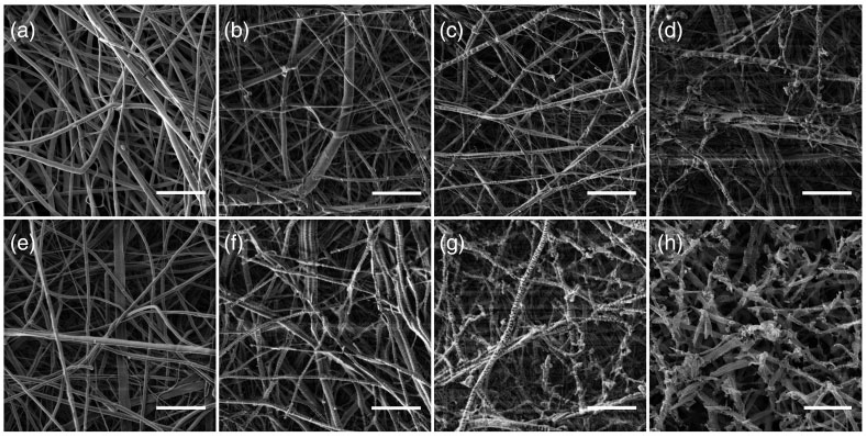

Figure 3. SEM images of PLA membranes of fiber density 16 g/m^2 before (a) and after plasma treatment with various power and exposure times: (b) 50 W 30 s, (c) 50 W 60 s, (d) 50 W 120 s, (e) 75 W 30 s, (f) 100 W 30 s, (g) 100 W 60 s, (h) 100 W 120 s. FE-SEM Tescan MIRA3, objective magnification 10,000×, bar 5μm.

by plasma treatment (plasma power 75 W, exposure time 30 s), and by the conditions under which the mechanical properties were measured (dry or wet conditions) (Table 2). The membranes are mainly used under wet conditions (e.g. immersed in a cell culture medium). These conditions are therefore more relevant for investigating the mechanical properties of the membranes. The dry non-treated membranes displayed elasto-plastic behavior with two different response areas. Young's modulus (E1) in the initial elastic area ($\varepsilon_{el} < 10$ %) and Young's modulus (E2) in the area of high deformations showed that the 16 g/m^2 and 5 g/m^2 fiber density membranes exhibit no difference in stiffness (Table 2) in both areas. The dry membranes became very brittle after plasma treatment, i.e. there was a significant increase in stiffness and no deformation response above ε_{el}, and therefore zero value for Young's modulus E2. The wet non-treated membranes displayed elasto-plastic behavior too, but with a significant decrease at ultimate tensile strength (TS). However, the maximum deformation (ε_{max}) did not change significantly compared to the dry membranes. The trend of the response to stress for the wet 5 g/m^2 plasma-treated membranes was similar to the trend for dry plasma-treated membranes; an even more brittle response with low ultimate strength and almost no deformation. The results for 16 g/m^2 indicate no significant difference between dry plasma-treated and wet plasma-treated membranes.

The changes in the surface elemental composition of the membrane after plasma treatment at various plasma power and exposure times were observed by

Table 2. Young's modulus E1 and E2, ultimate tensile strength TS and maximal deformation ε_{max} of PLA nanofiber membranes of different densities show the dependence of the mechanical response on the different treatment conditions.

	E1 (N/mm^2)			E2 (N/mm^2)			TS (N/mm^2)			ε_{max} (%)		
	Mean	SD	p	Mean	SD	p	Mean	SD	p	Mean	SD	p
5 vs	5.09	0.251	No	0.35	0.016	No	38.97	2.455	No	68.17	3.680	***
16 g/m^2	4.91	0.240		0.35	0.019		36.89	1.948		62.26	2.201	
5 TR vs	12.38	0.090	*	0.00	0.00	–	60.23	4.591	**	7.54	0.563	No
16 g/m^2 TR	7.65	0.824		0.00	0.00		37.79	3.467		8.74	0.409	
5 W vs	3.78	0.865	No	0.26	0.012	No	33.27	2.968	***	67.16	12.254	No
16 g/m^2 W	2.62	0.518		0.24	0.005		24.32	6.270		55.20	5.610	
5 TRW vs	5.68	0.725	No	0.00	0.00	–	19.65	4.270	***	4.43	1.655	–
16 g/m^2 TRW	8.88	0.842		0.00	0.00		44.81	4.283		12.03	2.045	

TR: plasma-treated membranes; W: wet membranes; p – p-value less than the significant level.
*$p < 0.001$.
**$p < 0.01$.
***$p < 0.05$
No ≥ 0.05.

Table 3. Concentration (in at.%) of carbon (C), oxygen (O) and groups C–C, C–O, C = O, determined by XPS on PLA nanofibers of fiber density 16 g/m^2 before (Pristine) and after plasma treatment with power 50–100 W and exposure time 30–120 s.

			C1s		
Sample	C (at.%)	O (at.%)	C–C	C–O	C = O
Pristine	63.8	36.2	39.1	13.9	10.8
50 W 30 s	61.5	38.5	31.7	14.0	15.9
50 W 60 s	60.0	40.0	30.8	15.4	13.7
50 W 120 s	60.0	40.0	27.7	15.3	17.0
75 W 30 s	63.1	36.9	36.8	13.4	12.9
100 W 30 s	62.5	37.5	33.9	14.3	14.3
100 W 60 s	58.7	41.3	30.2	13.3	15.2
100 W 120 s	62.5	37.5	34.5	13.9	14.1

X-ray photoelectron spectroscopy (XPS) (Table 3). The concentration of oxygen and oxygen-containing groups C–O and C = O was mainly determined, because the gas used for plasma discharge was oxygen, which incorporated into and reacted with the membrane surface. The concentration of oxygen was only slightly increased. The concentration of oxygen in non-treated (Pristine) PLA was relatively high, and thus the oxygen incorporated into the membrane surface after plasma treatment probably did not significantly influence the total oxygen concentration. The concentration of oxygen containing groups, mainly C = O, was increased after plasma treatment, but there was no significant dependence on plasma power or exposure time.

Adhesion and growth of HaCaT keratinocytes on polylactide nanofibrous membranes

Cell adhesion, growth, metabolic activity, morphology, and phenotypic maturation on PLA membranes of various fiber densities treated under the same plasma conditions. Nanofibrous membranes of different fiber densities (5, 9, 16 and 30 g/m^2) exposed to a plasma discharge with defined power 75 W and exposure time 30 s strongly influenced the cell behavior. The results indicate that in all three time intervals of cell cultivation, the amount of cell DNA, which correlates with the cell number, was significantly higher on plasma-treated membranes of almost all densities (Figure 4(a) to (c)). In addition, the XTT assay, which determined higher cell mitochondrial enzyme activity on plasma-treated membranes on day 3 after cell seeding, confirmed the positive effect of plasma treatment on cell behavior (Figure 4d). We also observed differences in the cell morphology and the cell cluster spreading area on plasma-treated and non-treated PLA membranes. At first, keratinocytes naturally adhered in clusters and then spread on the whole surface of the material. After a three-day cultivation, the cell cluster area was significantly larger on plasma-treated membranes than on non-treated membranes, with the exception of the membranes with the highest fiber density 30 g/m^2 – there was no significant difference between non-treated and plasma-treated samples (Figures 5 and 6).

The results also showed the influence of the membrane fiber densities on the amount of cell DNA, the cell population density, and the cell morphology. The amount of cell DNA was significantly higher on membranes of lower fiber densities (5 and 9 g/m^2) than on

membranes of higher fiber densities (16 and 30 g/m^2). These differences were clearer on plasma-treated membranes than on non-treated membranes (Figure 4(a) to (c)). The cell cluster area measured on day 3 was not significantly different on non-treated membranes of various fiber densities. However, on plasma-treated membranes of various fiber densities, the cells adhered in larger clusters on PLA membranes with fiber densities of 5 and 9 g/m^2 than on membranes with fiber densities of 16 and 30 g/m^2 (Figures 5 and 6).

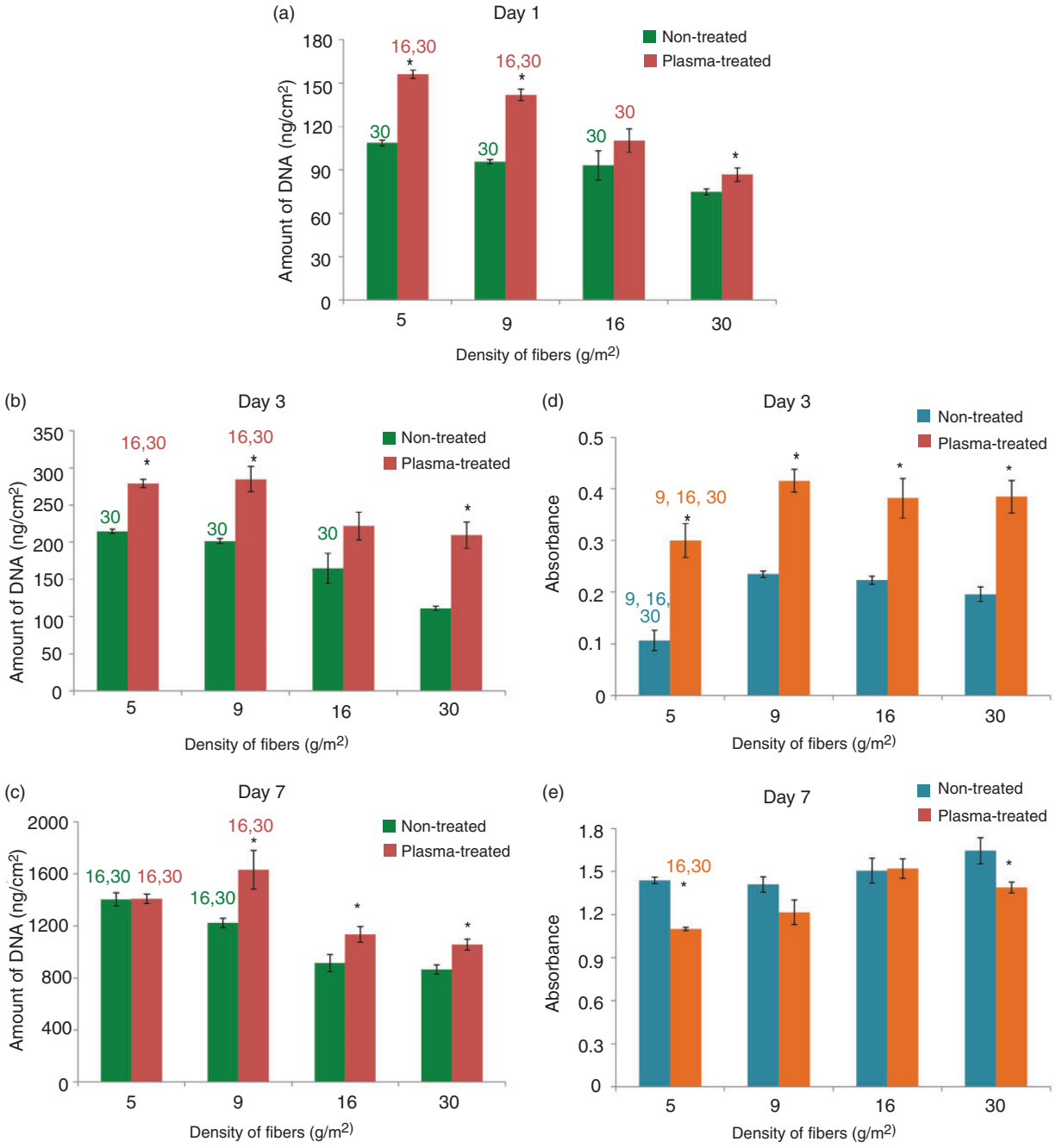

Figure 4. Amount of cell DNA measured by the Picogreen assay kit (a–c) and mitochondrial activity determined by the XTT assay kit (d, e) in human HaCaT keratinocytes on days 1, 3, and 7 on non-treated and plasma-treated (power 75 W, exposure time 30 s) PLA membranes of various fiber density (5, 9, 16, 30 g/m^2). Arithmetic means ± S.E.M. from nine measurements made on three independent samples for each experimental group and time interval. ANOVA, Student–Newman–Keuls method, statistical significance ($p \leq 0.05$): 5, 9, 16, 30 in comparison with the experimental group of the same label and * in comparison with the non-treated sample of the same fiber density.

Scanning electron microscopy, performed on days 3 and 7 after seeding (Figure 7), revealed that the HaCaT cells formed islands located predominantly on top of the nanofibrous membranes. However, in some places, fibers running through or above the cell islands were also observed. On day 7, the cell islands were considerably larger, so that large areas on the nanofibrous membranes were covered with cells, particularly in the case of the plasma-treated membranes (Figure 7(d) and (h)).

On day 3 after cell seeding, we investigated markers for the early and middle stage of keratinocyte differentiation (keratin 5, filaggrin, respectively) and molecules that play an important role in cell adhesion ($ß_1$ integrin receptors, vinculin and actin in the filamentous form, i.e. F-actin) (Figure 8). Immunofluorescence staining showed that the cells had well-developed keratin filaments on non-treated and plasma-treated membranes, and particularly on the control microscopic glass coverslips. On both types of nanofibrous membranes, keratin was located mainly at the cell periphery, while on the glass coverslips the keratin filaments were distributed throughout the entire cells. Filaggrin seemed to be present in a higher quantity on the PLA membranes than on the control glass. The cells adhered well through the adhesion receptors of the $ß_1$ integrin family on both types of PLA membranes and also on the control glass, where they showed a brighter fluorescence signal. Vinculin was distributed diffusely throughout all the cells or was organized into focal adhesion plaques, which were more apparent in the cells on the glass control. F-actin in cells on non-treated membranes, on plasma-treated membranes, and on the control glass was organized into fine fibers running in parallel between the opposite cell edges. These fibers were more apparent in the cells on the control glass, while on the nanofibrous membranes F-actin formed only tiny filaments or was distributed diffusely without forming specific fiber structures.

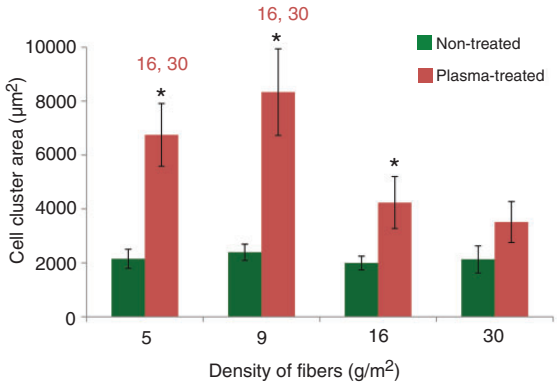

Figure 5. Cell cluster spreading area of HaCaT keratinocytes on day 3 on non-treated and plasma-treated (power 75 W, exposure time 30 s) PLA membranes of various fiber densities (5, 9, 16, 30 g/m^2), measured using Atlas software (Tescan Ltd., Brno, Czech Republic). Arithmetic means ± S.E.M. from 44 to 179 measurements. ANOVA, Student–Newman–Keuls method, statistical significance ($p \leq 0.05$): 5, 9, 16, 30 in comparison with the experimental group of the same label and * in comparison with the non-treated sample of the same fiber density.

Cell adhesion, growth, and morphology on PLA membranes treated under various plasma conditions. In this part of the study, we investigated the influence of various plasma conditions, i.e. various power and exposure times, on cell behavior. First, we treated membranes of fiber density 9 g/m^2 in plasma with power 25 W or 50 W and exposure times from 10 s to 30 s. Then we used higher power from 50 W to 100 W and longer exposure times from 30 s to 120 s. For plasma treatment with higher power and longer exposure times, we used membranes of higher fiber density (16 g/m^2), because more intense plasma treatment parameters (e.g. 100 W, 100 s) could cause serious degradation of membranes of lower fiber density.

Using lower power 25 W or 50 W and exposure times from 10 s to 30 s, we found a significantly higher

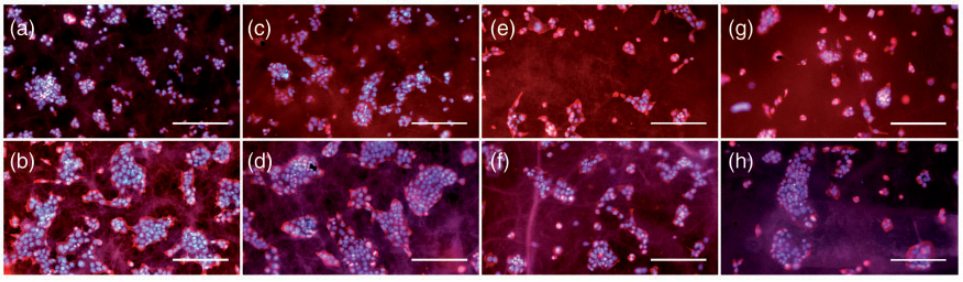

Figure 6. Morphology of human HaCaT keratinocytes after three-day cultivation on non-treated (a, c, e, g) and plasma-treated (power 75 W, exposure time 30 s; b, d, f, h) PLA membranes of various fiber densities (a, b: 5 g/m^2; c, d: 9 g/m^2; e, f: 16 g/m^2, g, h: 30 g/m^2). Cells stained with Texas Red C_2-Maleimide and Hoechst #33342. Olympus IX 51 microscope, obj. 10×, DP 70 digital camera, bar 200 μm.

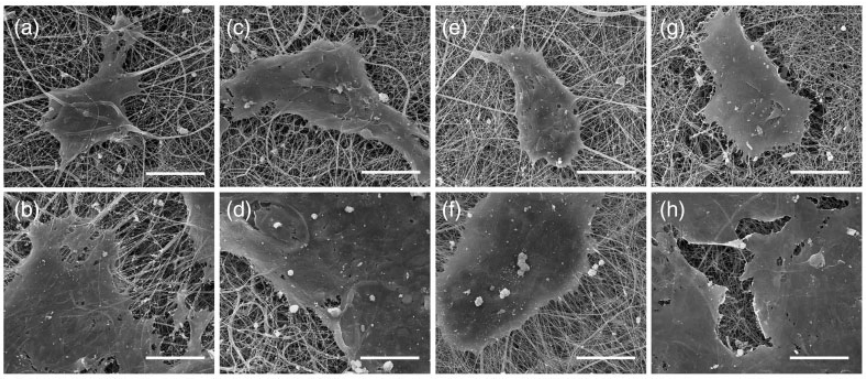

Figure 7. SEM images of the morphology of human HaCaT keratinocytes after three-day cultivation (a, c, e, g) and seven-day cultivation (b, d, f, h) on non-treated (a, b, e, f) and plasma-treated (power 75 W, exposure time 30 s; c, d, g, h) PLA membranes of fiber densities 5 g/m^2 (a–d) and 16 g/m^2 (e–h). Quanta 450 scanning electron microscope (FEI, USA), magnification 2000×, bar 40 μm.

amount of cell DNA, related to the cell number, on all plasma-treated samples than on the non-treated samples only on day 1 (Figure 9a), and on some samples on day 3 after cell seeding (Figure 9b). On day 7 after cell seeding, there were no significant differences in the amount of cell DNA between plasma-treated and non-treated membranes (Figure 9c). However, when we increased the plasma power (50–100 W) and the exposure time (30–120 s), we observed differences of higher significance between plasma-treated and non-treated membranes. On all plasma-treated samples, the cells adhered in higher population densities (as indicated by a higher amount of cell DNA) than on the non-treated samples on days 1 and 3 after seeding (Figure 9 (d) and (e)). On day 7 after seeding, significant differences in cell density between plasma-treated and non-treated membranes were found only on samples treated with power 50 W for 30 s and with power 75 W for 30 s (Figure 9f). Concerning the influence of various plasma conditions – power and exposure time – on the amount of cell DNA, we observed significant differences only among some plasma-treated samples (Figure 9(b), (d) and (f)).

The cell morphology and the size of the cell cluster spreading area on the non-treated and plasma-treated membranes showed a similar trend as the cell number (estimated by the amount of cell DNA). Using lower power (25 W, 50 W) and a shorter exposure time (10–30 s), we observed no differences between plasma-treated and non-treated samples in the cell morphology and the size of the cell cluster spreading area (Figures 10(a) and 11). However, an increase in power and exposure time led to a larger cell cluster area on plasma-treated membranes than on non-treated membranes (Figures 10(b) and 12). The difference in the cell cluster area was not significant between plasma-treated samples with various powers and exposure times.

Discussion

In the first part of the study, we investigated the influence of oxygen plasma and fiber density on the physical and chemical properties of nanofibrous membranes and on the behavior of human HaCaT keratinocytes in cultures on these materials. We observed a higher amount of cell DNA (which correlates with cell population density), higher cell metabolic activity, and larger size of the cell clusters (i.e. islands of cells) on plasma-treated membranes than on non-treated membranes. It was previously reported that plasma treatment changed the chemical and physical properties of the material surface. These alterations are induced by polymer chain degradation,[29] followed by the creation of free radicals and crosslinking between polymer chains. These primary changes lead to the formation of oxygen-containing groups. The oxidized groups enhance material surface wettability and promote adsorption of cell adhesion-mediating molecules in an appropriate spatial conformation. The specific amino acid sequences in these molecules (e.g. RGD) are therefore well accessible for cell adhesion receptors, and the cells can adhere and spread on the material by a considerably large area.[1] In our study, XPS analysis showed that the concentration of oxygen-containing groups, mainly C=O groups, had increased after the oxygen plasma treatment, which could lead to an increase in surface wettability. These changes in the physical properties of the surface could enhance cell adhesion and proliferation. Many previous studies have described a positive effect of plasma treatment on the adhesion and growth of a variety of cells. For example, Gugala and Gogolewski reported that oxygen plasma treatment increased the wettability and the concentration of oxygen on the surface of PLA porous membranes. These changes enhance the attachment and growth of osteoblasts.[30]

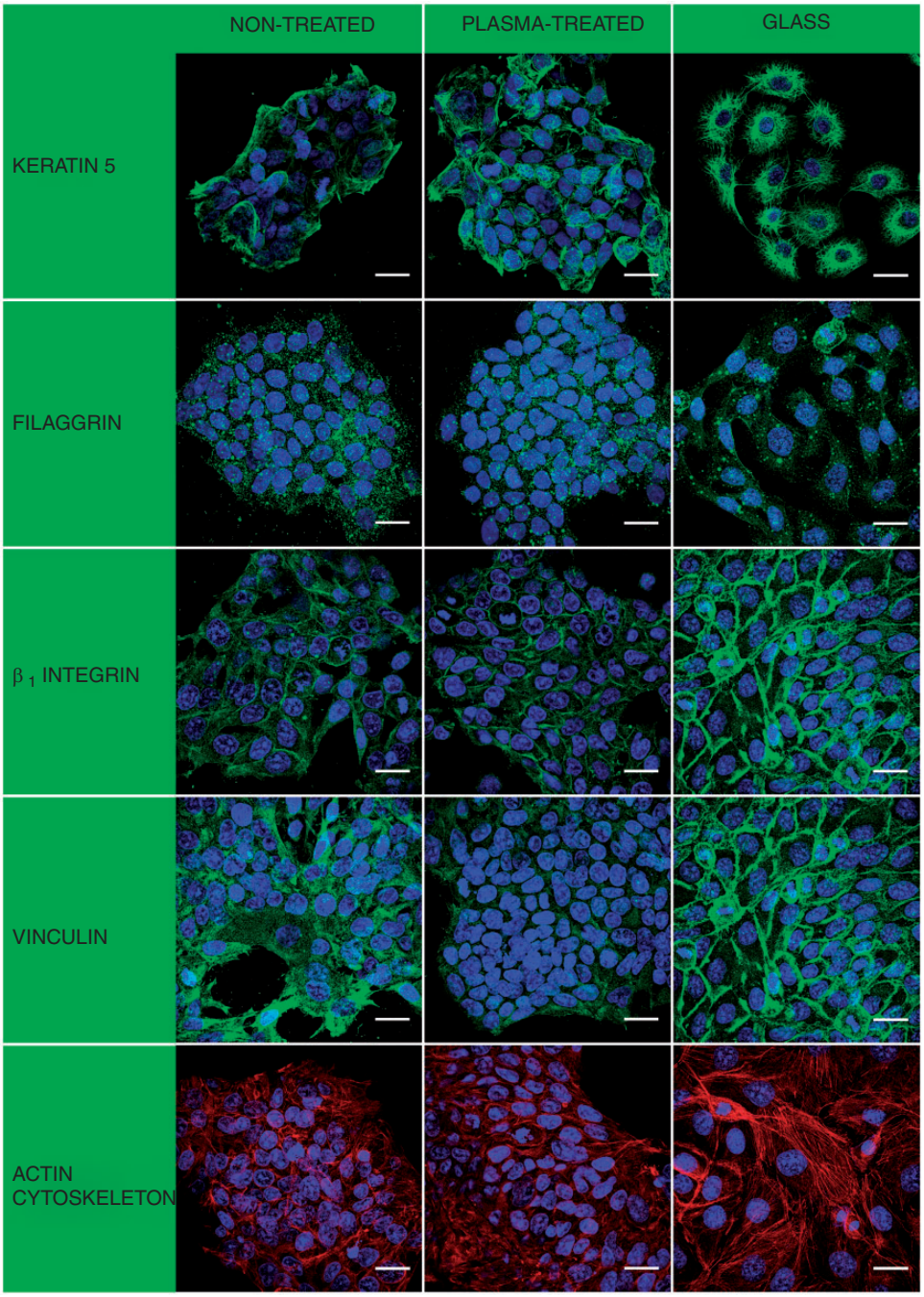

Figure 8. Immunofluorescence staining of cytokeratin 5 and filaggrin (differentiation markers of keratinocytes), β_1 integrin adhesion receptors and vinculin (an integrin-associated protein of focal adhesion plaques), phalloidin staining of F-actin (filamentous cytoskeletal protein) and cell nucleus staining (Hoechst 33342, blue) in human HaCaT keratinocytes after three days of cultivation on non-treated and plasma-treated (power 75 W, exposure time 30 s) PLA membranes of fiber density 9 g/m^2 and on control microscopic glass coverslips (glass). Leica TCS SPE DM2500 confocal microscope, obj. 63 × /1.3 NA oil, bar 25 μm.

Wan *et al*. treated poly (lactide-*co*-glycolide) films (PLGA) with oxygen plasma, and they observed the incorporation of polar groups into the material surface, an increase in its hydrophilicity, and the promotion of adhesion and growth of mouse fibroblasts.[31] Jeong et al. enhanced the cellular activity of human epidermal keratinocytes and fibroblasts by exposing silk fibroin nanofibers to oxygen plasma. The adhesion of the cells was promoted by an increase in the hydrophilicity of the material surface after plasma treatment.[32] Other factors that might improve cell adhesion and growth on plasma-modified nanofibers are an increase in overall

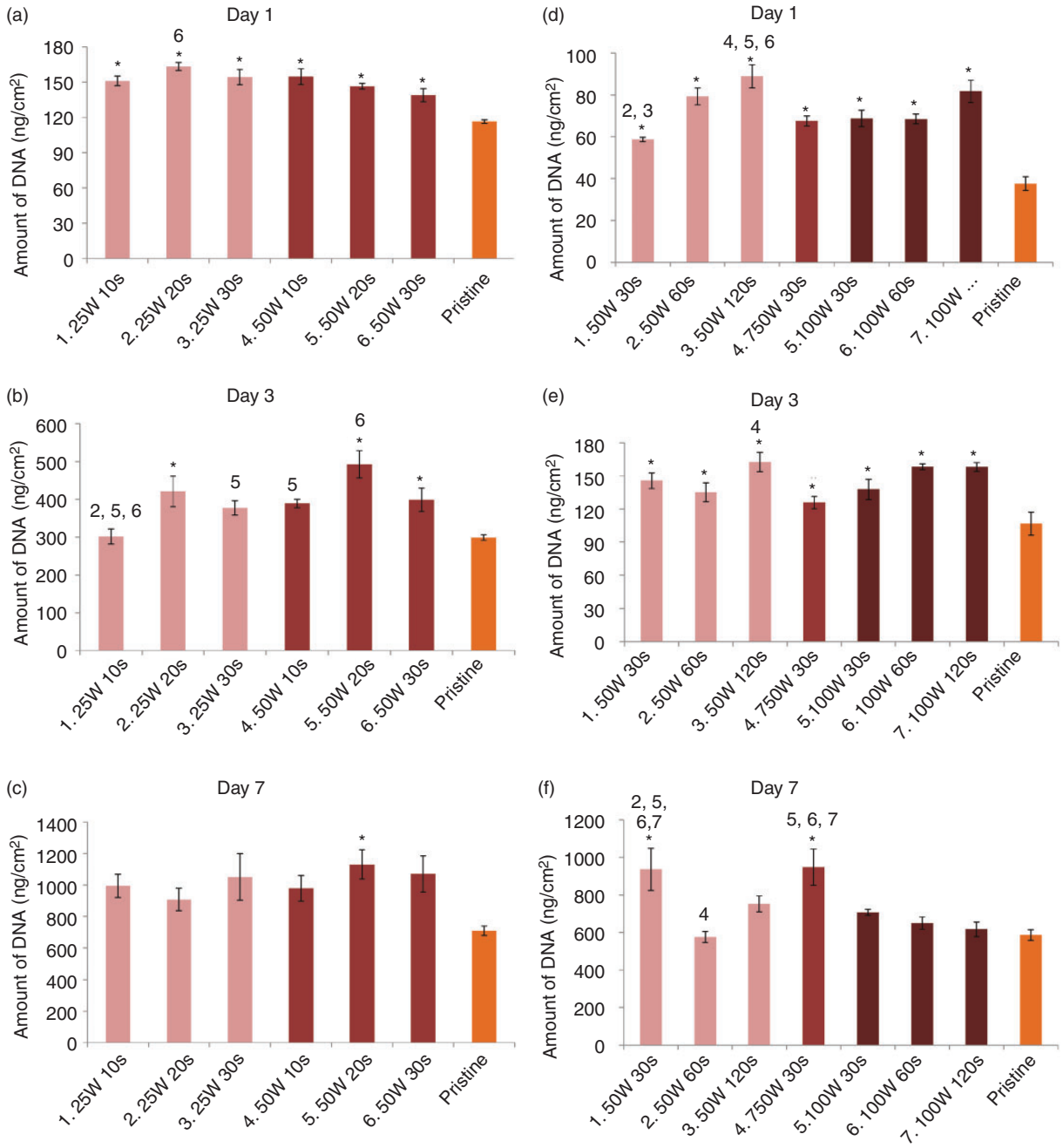

Figure 9. Amount of cell DNA measured by the Picogreen assay kit in human HaCaT keratinocytes on days 1, 3, and 7 on non-treated (Pristine) and plasma-treated (various power 25–50 W and 50–100 W, exposure time 10–30 s and 30–120 s) PLA membranes with fiber density 9 g/m^2 (a–c) and 16 g/m^2 (d–f). Arithmetic means ± S.E.M. from nine measurements made on three independent samples for each experimental group and time interval. ANOVA, Student–Newman–Keuls method, statistical significance ($p \leq 0.05$) in comparison with a certain experimental group are indicated by the number of the group above the column and * in comparison with the non-treated sample (Pristine).

material stiffness and the formation of an additional nanostructure on the material surface. Our earlier studies performed on plasma-treated polymeric foils revealed newly formed nanoscale irregularities on foils that were originally flat, due to partial degradation of the foil surface.[24,25] Also in this study, SEM imaging revealed degradation of the fiber surface, at least at higher plasma powers and longer exposure times. It has been repeatedly shown that the surface nanostructure of various materials has beneficial effects on cell

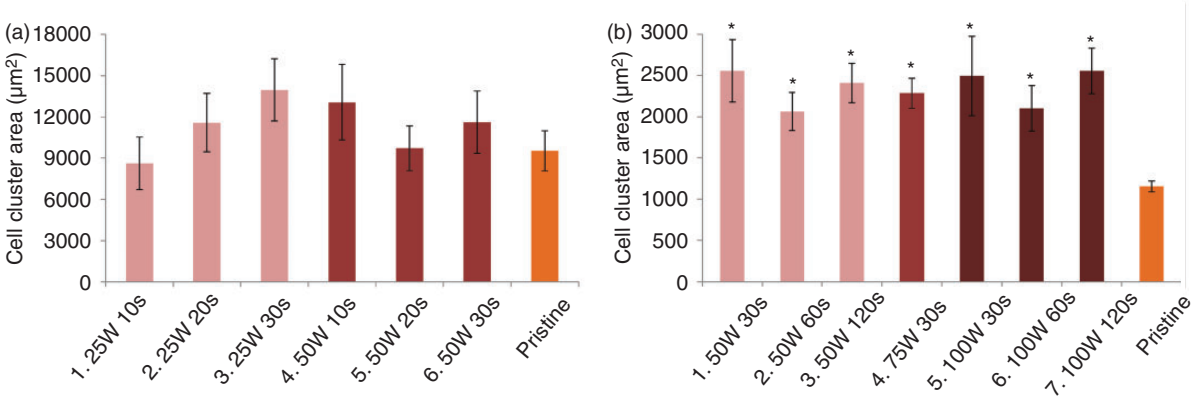

Figure 10. Cell cluster spreading area of HaCaT keratinocytes on day 3 on non-treated and plasma-treated samples (various power 25–50 W and 50–100 W, exposure time 10–30 s and 30–120 s) PLA membranes of fiber density 9 g/m^2 (a) and 16 g/m^2 (b) measured using Atlas software (Tescan Ltd., Brno, Czech Republic). Arithmetic means ± S.E.M. from 44 to 274 measurements. ANOVA, Student-Newman–Keuls method, statistical significance ($p \leq 0.05$): * in comparison with the non-treated sample.

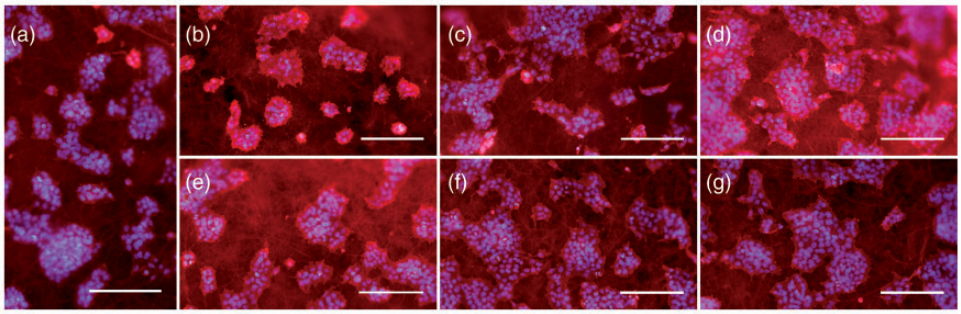

Figure 11. Morphology of human HaCaT keratinocytes after three-day cultivation on non-treated (a) and plasma-treated PLA nanofibers of fiber density 9 g/m^2: (b) 25 W 10 s, (c) 25 W 20 s, (d) 25 W 30 s, (e) 50 W 10 s, (f) 50 W 20 s, (g) 50 W 30 s. Cells stained with Texas Red C_2-Maleimide and Hoechst #33342. Olympus IX 51 microscope, obj. 10×, DP 70 digital camera, bar 200 μm.

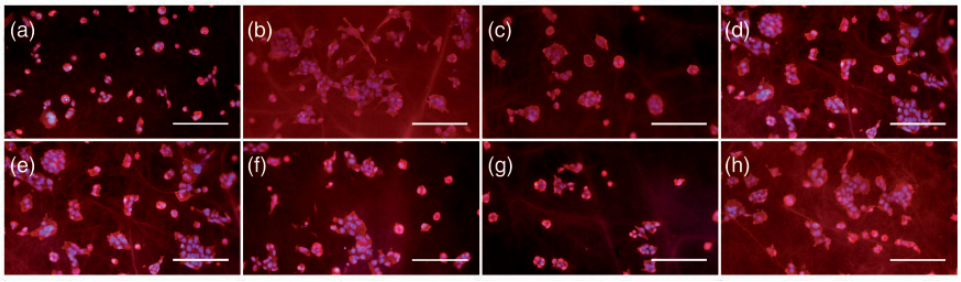

Figure 12. Morphology of human HaCaT keratinocytes after three-day cultivation on non-treated (a) and plasma-treated PLA nanofibrous membranes of fiber density 16 g/m^2: (b) 50 W 30 s, (c) 50 W 60 s, (d) 50 W 120 s, (e) 75 W 30 s, (f) 100 W 30 s, (g) 100 W 60 s, (h) 100 W 120 s. Cells stained with Texas Red C_2-Maleimide and Hoechst #33342. Olympus IX 51 microscope, obj. 10×, DP 70 digital camera, bar 200 μm.

adhesion and growth, which can act synergistically with the material wettability.[1,20]

However, as revealed by immunofluorescence, the plasma treatment appeared to have no significant influence on the presence and distribution of molecular markers of cell adhesion and spreading, namely β_1-integrins, vinculin, and F-actin. The staining pattern of these molecules was similar in cells on non-treated nanofibrous membranes and on plasma-treated nanofibrous membranes. However, this pattern differed

between the cells on nanofibrous membranes and on the control glass coverslips. On the glass coverslips, the intensity of the fluorescence of the β_1-integrins and vinculin was higher, and the F-actin filaments were better developed. Similarly, filamentous organization of keratin 5 was also more apparent on the glass coverslips. This could be explained by the fact that the glass coverslips provided firmer and more continuous support for cell attachment than the relatively loose and porous nanofibrous network, which may not provide sufficient surface area for cell adhesion and spreading.[33] On the other hand, the immunofluorescence of filaggrin in cells on nanofibrous membranes, particularly on less stiff non-treated membranes, appeared brighter than on the glass coverslips. Filaggrin is a structural protein involved in the mechanical resistance and integrity of an epithelial barrier,[34] and this barrier function is probably more difficult to maintain on relatively weak nanofibrous membranes.

Although HaCaT keratinocytes are an immortalized cell line, they conserved markers of keratinocyte differentiation, including markers of terminal keratinocyte differentiation (keratins 1 and 10),[35] late markers involucrin[36] and loricrin,[37] an intermediate marker filaggrin,[38] and an early marker keratin 5.[39,40] In the physiological skin, the terminal, late, and intermediate markers are expressed in suprabasal layers of keratinocytes (i.e. spinous and granular layers), while cytokeratin 5 is expressed in the basal layer.[37,40,41] The expression of differentiation markers in HaCaT cells is influenced by various factors, such as cell population density,[41] the composition of the cell culture media, particularly the concentration of calcium,[36] and also by the time of cultivation.[42] In our system with 7-day cultivation of HaCaT cells on nanofibrous meshes or on glass coverslips, immunofluorescence revealed almost no cytokeratins 1 and 10 (data not shown) but relatively bright signals for keratin 5 and filaggrin, which suggested an early or middle stage of HaCaT cell differentiation. However, immunofluorescence staining did not show striking differences in the presence and distribution of keratin 5 and fillagrin in cells on non-treated and plasma-treated nanofibrous membranes. Therefore, there is a need for a further, deeper investigation, e.g. by biochemical methods capable of quantifying these molecules at protein and mRNA level.

Fiber density had a significant effect on the adhesion and growth of cells. We measured a higher amount of cell DNA, cell metabolic activity and a larger cell cluster spreading area on membranes with lower fiber densities (5 or 9 g/ m^2) than on membranes with higher fiber densities (16 or 30 g/m^2). This effect was more apparent on plasma-treated membranes. Soliman et al. reported on the effect of the fiber packing density of nanofibrous membranes on cell behavior. They showed the dependence of pore size on the fiber packing density and its subsequent effect on cell behavior. Higher fiber packing density resulted in smaller pores and weaker cell proliferation.[33] We observed similar results mainly on plasma-treated membranes. The area of void spaces between the fibers of the membranes increased with decreasing fiber density, which led to better cell adhesion and proliferation. Larger spaces between fibers may have provided more space for the cells to proliferate and migrate into a deeper layer of the membranes. They may also enable a better supply of oxygen and nutrients for the cells, and quicker waste removal.[33] However, the area of void spaces between fibers decreased significantly after plasma treatment, which further enhanced the dependence of cell adhesion and growth on the fiber density of the membranes. Smaller spaces between fibers on plasma-treated membranes of higher fiber densities probably led to significantly lower cell colonization of these membranes. This insufficiency may also have been caused by a decrease in mechanical deformability, and by an increase in the rigidity and fragility of the plasma-treated membranes. In addition, according to SEM analysis, significantly stronger modification of nanofibers of higher fiber densities may not provide sufficient support for cell adhesion and proliferation.

In the second part of the study, we investigated the effect of various plasma conditions (plasma power and exposure time) on altering the physical and chemical properties of the polymer surface, and its influence on cell adhesion and growth. SEM analysis showed that when plasma power less than 50 W and exposure time shorter than 30 s were used, there was no modification of the membranes. However, if higher power (from 50 W to 100 W) and a longer exposure time (from 30 s to 120 s) were applied, the modification of the fibers increased with plasma power and exposure time. We observed that the plasma exposure time seemed to have a more significant effect on the modification and degradation of the fibers. Wan et al. had similar results when they treated a porous PLA scaffold with NH_3 plasma. They showed that the depth of the modification of the scaffold increased mainly with exposure time, while degradation of the scaffold increased with increasing exposure time and plasma power.[43]

Cells cultivated on membranes treated under mild plasma conditions (plasma power less than 50 W and exposure time shorter than 30 s) did not show significantly better adhesion, proliferation, or a larger area of cell clusters than non-treated membranes. As mentioned earlier, SEM analysis did not reveal any significant alteration in the morphology of membranes treated under mild plasma conditions. It therefore seems that these mild plasma treatment conditions did

not have a significant effect on the physical and chemical composition of the membrane surface and on the cell behavior. However, stronger plasma treatment (plasma power ranging from 50 W to 100 W and exposure time ranging from 30 s to 120 s) enhanced cell attachment, proliferation, and spreading in comparison with non-treated membranes. However, we observed no significant dependence of cell behavior on modulation of plasma power and exposure time. XPS analysis showed a slight increase in polar groups on the material surface after plasma treatment, but did not show significant differences in surface chemical composition depending on plasma power and exposure time. This observation indicates that an increase in plasma power and exposure time above a specific effective plasma treatment condition limit does not have a significant influence on cell behavior. The effect of different plasma conditions, plasma power, and exposure time on cell behavior would be more pronounced when there is dynamic cultivation of the cells. Wan et al. showed that different exposure times had a different influences on the detachment of cells enduring shear stress during dynamic cultivation on the material.[44]

Conclusion

Oxygen plasma treatment of PLA nanofibrous membranes had a positive influence on cell colonization of the material. The beneficial effect of plasma treatment on cell adhesion and growth could be attributed to the formation of new oxidized structures on the membrane surface, an increase in surface wettability, and an increase in surface stiffness. No clear dependence of cell behavior on different plasma conditions (plasma power and exposure time) was observed, though higher plasma power and, in particular, longer exposure times resulted in more pronounced improvement of the cell adhesion and growth. The fiber density of the membranes also played an important role in cell adhesion and growth. The cells preferentially adhered to membranes of lower fiber densities, probably due to the larger void spaces between the fibers. This effect was more pronounced on plasma-treated membranes than on non-treated membranes. Thus, PLA nanofibrous membranes are promising materials for the construction of temporary carriers for skin cells, particularly after physical modifications are made to them.

Acknowledgements

The authors would like to acknowledge the kind assistance of Dr Jitka Libertinova (Inst. of Physics, Acad. Sci. CR) for SEM of the nanofiber morphology and Mr Robin Healey (Czech Technical University in Prague) for his language revision of the manuscript.

Declaration of conflicting interests

None declared.

Funding

This study was supported by the Grant Agency of the Czech Republic (grant No. P108/12/G108). Further financial support was provided by the "BIOCEV – Biotechnology and Biomedicine Centre of the Academy of Sciences and Charles University" (CZ.1.05/1.1.00/02.0109), project from the European Regional Development Fund.

References

1. Bacakova L, Filova E, Parizek M, et al. Modulation of cell adhesion, proliferation and differentiation on materials designed for body implants. *Biotechnol Adv* 2011; 29: 739–767.
2. Parizek M, Douglas TE, Novotna K, et al. Nanofibrous poly(lactide-co-glycolide) membranes loaded with diamond nanoparticles as promising substrates for bone tissue engineering. *Int J Nanomed* 2012; 7: 1931–1951.
3. Auxenfans C, Fradette J, Lequeux C, et al. Evolution of three dimensional skin equivalent models reconstructed in vitro by tissue engineering. *Eur J Dermatol* 2009; 19: 107–113.
4. Prasitsilp M, Siriwittayakorn T, Molloy R, et al. Cytotoxicity study of homopolymers and copolymers of 2-hydroxyethyl methacrylate and some alkyl acrylates for potential use as temporary skin substitutes. *J Mater Sci Mater Med* 2003; 14: 595–600.
5. Young CD, Wu JR and Tsou TL. High-strength, ultrathin and fiber-reinforced pHEMA artificial skin. *Biomaterials* 1998; 19: 1745–1752.
6. El-Ghalbzouri A, Lamme EN, van Blitterswijk C, et al. The use of PEGT/PBT as a dermal scaffold for skin tissue engineering. *Biomaterials* 2004; 25: 2987–2996.
7. Malin EW, Galin CM, Lairet KF, et al. Silver-coated nylon dressing plus active DC microcurrent for healing of autogenous skin donor sites. *Ann Plast Surg* 2013; 71: 481–484.
8. Marston WA, Hanft J, Norwood P, et al. The efficacy and safety of dermagraft in improving the healing of chronic diabetic foot ulcers: results of a prospective randomized trial. *Diabetes Care* 2003; 26: 1701–1705.
9. Peschel G, Dahse HM, Konrad A, et al. Growth of keratinocytes on porous films of poly(3-hydroxybutyrate) and poly(4-hydroxybutyrate) blended with hyaluronic acid and chitosan. *J Biomed Mater Res A* 2008; 85: 1072–1081.
10. Dai NT, Williamson MR, Khammo N, et al. Composite cell support membranes based on collagen and polycaprolactone for tissue engineering of skin. *Biomaterials* 2004; 25: 4263–4271.
11. Selig HF, Keck M, Lumenta DB, et al. The use of a polylactide-based copolymer as a temporary skin substitute in deep dermal burns: 1-year follow-up results of a prospective clinical noninferiority trial. *Wound Repair Regen* 2013; 21: 402–409.

12. Chen G, Sato T, Ohgushi H, et al. Culturing of skin fibroblasts in a thin PLGA-collagen hybrid mesh. *Biomaterials* 2005; 26: 2559–2566.
13. Pajoum Shariati SR, Shokrgozar MA, Vossoughi M, et al. In vitro co-culture of human skin keratinocytes and fibroblasts on a biocompatible and biodegradable scaffold. *Iran Biomed J* 2009; 13: 169–177.
14. Ma L, Gao C, Mao Z, et al. Collagen/chitosan porous scaffolds with improved biostability for skin tissue engineering. *Biomaterials* 2003; 24: 4833–4841.
15. Morimoto N, Suzuki S, Kim BM, et al. In vivo cultured skin composed of two-layer collagen sponges with preconfluent cells. *Ann Plast Surg* 2001; 47: 74–81.
16. Harris PA, di Francesco F, Barisoni D, et al. Use of hyaluronic acid and cultured autologous keratinocytes and fibroblasts in extensive burns. *Lancet* 1999; 353: 35–36.
17. Liu H, Mao J, Yao K, et al. A study on a chitosan-gelatin-hyaluronic acid scaffold as artificial skin in vitro and its tissue engineering applications. *J Biomater Sci Polym Ed* 2004; 15: 25–40.
18. Lacroix S, Bouez C, Vidal S, et al. Supplementation with a complex of active nutrients improved dermal and epidermal characteristics in skin equivalents generated from fibroblasts from young or aged donors. *Biogerontology* 2007; 8: 97–109.
19. Pandey AK. Recent advancements of biodegradable polylactic acid/ polylactide: A review on synthesis, characterization and applications. *Adv Mater* 2013 (in press).
20. Bacakova L and Svorcik V. Cell colonization control by physical and chemical modification of materials. In: Kimura D (ed.) *Cell growth processes: new research*. USA: Nova Science Publishers, Inc., 2008, pp.5–56.
21. Svorcik V, Rybka V, Hnatowicz V, et al. Structure and biocompatibility of ion beam modified polyethylene. *J Mater Sci Mater Med* 1997; 8: 435–440.
22. Walachova K, Svorcik V, Bacakova L, et al. Colonization of ion-modified polyethylene with vascular smooth muscle cells in vitro. *Biomaterials* 2002; 23: 2989–2996.
23. Heitz J, Svorcik V, Bacakova L, et al. Cell adhesion on polytetrafluoroethylene modified by UV-irradiation in an ammonia atmosphere. *J Biomed Mater Res A* 2003; 67: 130–137.
24. Novotna K, Bacakova M, Kasalkova N, et al. Adhesion and growth of vascular smooth muscle cells on nanostructured and biofunctionalized polyethylene. *Materials* 2013; 6: 1632–1655.
25. Parizek M, Slepickova Kasalkova N, Bacakova L, et al. Adhesion, growth, and maturation of vascular smooth muscle cells on low-density polyethylene grafted with bioactive substances. *BioMed Res Int* 2013; 2013: 1–18.
26. Pareta RA, Reising AB, Miller T, et al. Increased endothelial cell adhesion on plasma modified nanostructured polymeric and metallic surfaces for vascular stent applications. *Biotechnol Bioeng* 2009; 103: 459–471.
27. Kubies D, Rypacek F, Kovarova J, et al. Microdomain structure in polylactide-block-poly(ethylene oxide) copolymer films. *Biomaterials* 2000; 21: 529–536.
28. Boukamp P, Petrussevska RT, Breitkreutz D, et al. Normal keratinization in a spontaneously immortalized aneuploid human keratinocyte cell line. *J Cell Biol* 1988; 106: 761–771.
29. Nakagawa M, Teraoka F, Fujimoto S, et al. Improvement of cell adhesion on poly(L-lactide) by atmospheric plasma treatment. *J Biomed Mater Res A* 2006; 77: 112–118.
30. Gugala Z and Gogolewski S. Attachment, growth, and activity of rat osteoblasts on polylactide membranes treated with various low-temperature radiofrequency plasmas. *J Biomed Mater Res A* 2006; 76: 288–299.
31. Wan Y, Qu X, Lu J, et al. Characterization of surface property of poly(lactide-co-glycolide) after oxygen plasma treatment. *Biomaterials* 2004; 25: 4777–4783.
32. Jeong L, Yeo IS, Kim HN, et al. Plasma-treated silk fibroin nanofibers for skin regeneration. *Int J Biol Macromol* 2009; 44: 222–228.
33. Soliman S, Sant S, Nichol JW, et al. Controlling the porosity of fibrous scaffolds by modulating the fiber diameter and packing density. *J Biomed Mater Res A* 2011; 96: 566–574.
34. McGrath JA. Filaggrin and the great epidermal barrier grief. *Australas J Dermatol* 2008; 49: 67–73.
35. Prado E, Wurtz T, Ferbus D, et al. Sodium fluoride influences the expression of keratins in cultured keratinocytes. *Cell Biol Toxicol* 2011; 27: 69–81.
36. Micallef L, Belaubre F, Pinon A, et al. Effects of extracellular calcium on the growth-differentiation switch in immortalized keratinocyte HaCaT cells compared with normal human keratinocytes. *Exp Dermatol* 2009; 18: 143–151.
37. Breitkreutz D, Schoop VM, Mirancea N, et al. Epidermal differentiation and basement membrane formation by HaCaT cells in surface transplants. *Eur J Cell Biol* 1998; 75: 273–286.
38. Hong JH, Youm JK, Kwon MJ, et al. K6PC-5, a direct activator of sphingosine kinase 1, promotes epidermal differentiation through intracellular Ca2+ signaling. *J Invest Dermatol* 2008; 128: 2166–2178.
39. Zhou LL, Lin ZX, Fung KP, et al. Ethyl acetate fraction of Radix rubiae inhibits cell growth and promotes terminal differentiation in cultured human keratinocytes. *J Ethnopharmacol* 2012; 142: 241–247.
40. Kitagawa N, Inai Y, Higuchi Y, et al. Inhibition of JNK in HaCaT cells induced tight junction formation with decreased expression of cytokeratin 5, cytokeratin 17 and desmoglein 3. *Histochem Cell Biol* 2014; 1–11.
41. Poumay Y and Pittelkow MR. Cell density and culture factors regulate keratinocyte commitment to differentiation and expression of suprabasal K1/K10 keratins. *J Invest Dermatol* 1995; 104: 271–276.

42. Schoop VM, Mirancea N and Fusenig NE. Epidermal organization and differentiation of HaCaT keratinocytes in organotypic coculture with human dermal fibroblasts. *J Invest Dermatol* 1999; 112: 343–353.
43. Wan Y, Tu C, Yang J, et al. Influences of ammonia plasma treatment on modifying depth and degradation of poly(L-lactide) scaffolds. *Biomaterials* 2006; 27: 2699–2704.
44. Wan Y, Yang J, Yang J, et al. Cell adhesion on gaseous plasma modified poly-(l-lactide) surface under shear stress field. *Biomaterials* 2003; 24: 3757–3764.